



Cite this: *Energy Environ. Sci.*, 2016, 9, 3682

Received 2nd September 2016,  
Accepted 4th November 2016

DOI: 10.1039/c6ee02562e

www.rsc.org/ees

## A highly-robust solid oxide fuel cell (SOFC): simultaneous greenhouse gas treatment and clean energy generation†

T. Li,<sup>a</sup> M. F. Rabuni,<sup>a</sup> L. Kleiminger,<sup>a</sup> B. Wang,<sup>a</sup> G. H. Kelsall,<sup>a</sup> U. W. Hartley<sup>b</sup> and K. Li<sup>\*a</sup>

Herein, results of combined greenhouse gas treatment with clean energy conversion is reported for the first time. Multi-channel tubular SOFCs were operated with N<sub>2</sub>O instead of air as the oxidant leading to a 50% increase in power density. Techno-economic evaluation suggested the feasibility of the combined approach eliminating the cost penalty for N<sub>2</sub>O abatement.

With a global warming potential 298 times greater than that of CO<sub>2</sub>, N<sub>2</sub>O is one of the greenhouse gases contributing to ozone depletion and climate change.<sup>1–5</sup> N<sub>2</sub>O is released by both natural, *e.g.* microbial transformation of nitrogen in soil, and anthropogenic sources.<sup>6–8</sup> The main anthropogenic emission of the chemical industry comes from the manufacturing of adipic acid (C<sub>6</sub>H<sub>10</sub>O<sub>4</sub>) and nitric acid (HNO<sub>3</sub>), used as the feedstock in fertilizer and synthetic fiber production, in which N<sub>2</sub>O is generated as a by-product.<sup>9,10</sup>

To date, several technologies have been proposed to control the release of N<sub>2</sub>O from agricultural and industrial processes. For the former, the mitigation approaches often involve the use of soil microbes *via* biological processes.<sup>11,12</sup> Control measures in the production of adipic or nitric acid involve thermal/catalytic decomposition processes. The catalytic route can be selective or non-selective, *i.e.* the reaction with a fuel. The drawbacks of these are either the requirement of a high working temperature (> 1000 °C) to facilitate decomposition, *i.e.* a very energy intense process, or expensive catalysts with limited lifespans.<sup>13,14</sup>

Solid oxide fuel cells (SOFCs) can convert chemical to electrical energy cleanly and with higher efficiencies than conventional power plants.<sup>15,16</sup> The high operating temperatures (> 600 °C) provide enhanced kinetics and fuel flexibility.<sup>17–19</sup> The geometry of micro-tubular SOFCs has shown improved thermal shock

### Broader context

N<sub>2</sub>O has been identified as one of the most detrimental ozone-depletion substances, with a global warming potential (GWP) that is *ca.* 298 times greater than that of CO<sub>2</sub>. However, conventional industrial abatement processes (thermal or catalytic decomposition) require either high working temperatures (> 1000 °C) or expensive catalysts with limited lifespans. Solid oxide fuel cells (SOFCs) have been well established as one of the most promising technologies for clean electrical energy generation in the future. In this study, it was reported for the first time that SOFCs can be operated using N<sub>2</sub>O as the oxidant. A considerable improvement in cell performances of approximately 50% was observed when using N<sub>2</sub>O compared to conventionally used air. Such enhanced power output, together with N<sub>2</sub>O decomposition at intermediate temperatures (750 °C), indicates successful integration of clean energy conversion and greenhouse treatment. The techno-economic analysis suggested that this novel conceptual design may well eliminate the cost penalty for industrial N<sub>2</sub>O abatement.

resistance, simplified sealing and increased volumetric power densities.<sup>20,21</sup> However, this geometric design has yet to be commercialized, *inter alia* because of low mechanical strength,<sup>22</sup> as the long, slim micro-tubes are vulnerable to fracture by forces applied vertically on a longitudinal direction, which makes the micro-tubular SOFC stacks quite fragile to external vibrations. Therefore, the enhancement in mechanical strength is crucial before it can be applied in practical applications, such as an auxiliary power unit (APU) and a combined heat and power (CHP) system.

We report herein a new concept: operating SOFCs with nitrous oxide as an oxidant instead of conventionally used air. This combines the treatment of N<sub>2</sub>O as a greenhouse gas with clean electrical energy generation. A novel multi-channel tubular reactor design was utilized, providing enhanced mechanical strength. Results for fuel cell operation with air or nitrous oxide as the oxidant are presented, and the techno-economic aspects of the combined systems are discussed.

A schematic diagram of the multi-channel SOFC (for experimental fabrication process, see the ESI†) and the operating principle of the SOFC using N<sub>2</sub>O as an oxidant are depicted in Fig. 1a and b, respectively.

<sup>a</sup> Department of Chemical Engineering, Imperial College London, London, SW7 2AZ, UK. E-mail: Kang.li@imperial.ac.uk

<sup>b</sup> Chemical Process Engineering, The Srinthorn International Thai-German Graduate School of Engineering, King Mongkut's University of Technology North Bangkok, Bangkok 10800, Thailand

† Electronic supplementary information (ESI) available. See DOI: 10.1039/c6ee02562e



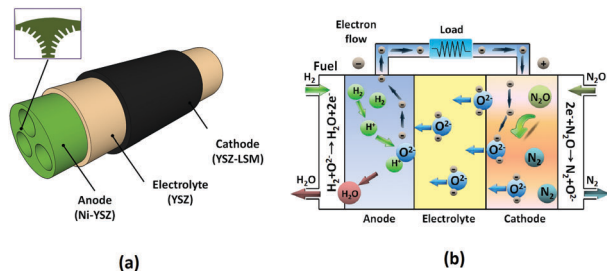


Fig. 1 (a) Schematic diagram of the multi-channel SOFC and materials for each component. The inset shows the pattern of the hierarchical asymmetric structure. (b) Schematic diagram of the working principle of SOFC running on N<sub>2</sub>O.

Nitrous oxide was fed to the cathode side, which has a bi-layer structure with a lanthanum strontium manganite (LSM)–yttria-stabilized zirconia (YSZ) inner layer (LSM/YSZ = 50/50 by weight) and a pure LSM outer layer for current collection. N<sub>2</sub>O was then decomposed catalytically into nitrogen and oxygen, the latter being reduced to oxide ions (O<sup>2-</sup>) and transported through the YSZ electrolyte.

Fig. 2 shows SEM images of the multi-channel anode and electrolyte (see the ESI† for images with higher magnifications showing the details of the micro-channels and sponge-like region). Uniform channels of the anode are produced using a specially designed spinneret (extruder) as shown in Fig. 2a. As the internal coagulant was split into three streams, several phase inversion processes occurred simultaneously, leading to the formation of a hierarchical asymmetric structure composed of micro-channels and sponge-like regions.<sup>23</sup> A well-tailored micro-structure can improve cell performances considerably.<sup>24</sup> The presence of micro-channels has been proven to facilitate mass transport rates, whereas the sponge-like region increases the densities of triple-phase boundaries (TPBs) where fuel oxidation occurs.<sup>23</sup> The dip-coated YSZ electrolyte was approximately 10 μm thick (Fig. 2b) and well densified after sintering at 1450 °C for 6 hours (Fig. 2c).

The nitrogen permeance at room temperature was determined to be of the order  $1 \times 10^{-11} \text{ mol m}^{-2} \text{ s}^{-1} \text{ Pa}^{-1}$ , implying suitable gas-tightness had been obtained for the YSZ electrolyte.<sup>25</sup> The fracture robustness of a 3-channel anode was investigated using three-point bending tests (for experimental details see the ESI†); the fracture load was measured as approximately 24 N, which is more than 3–4 times higher than that of single-channel counterparts fabricated under similar conditions.<sup>26</sup> Such marked enhancement in mechanical robustness could effectively facilitate stack assembly and improve the resistance towards external impact. Hence, this novel multi-channel design could be a promising solution to the long-existing problem of low mechanical strength that has hindered the micro-tubular SOFC design from wider applications.

The electrochemical performance was measured by supplying 30 ml min<sup>-1</sup> of pure hydrogen as the fuel and 50 ml min<sup>-1</sup> of oxidant (air, N<sub>2</sub>O or pure O<sub>2</sub>). As depicted in Fig. 3a–c, open-circuit potential differences (OCPDs) for various oxidants ranged between 1.15 and 1.17 V, which are relatively close to the

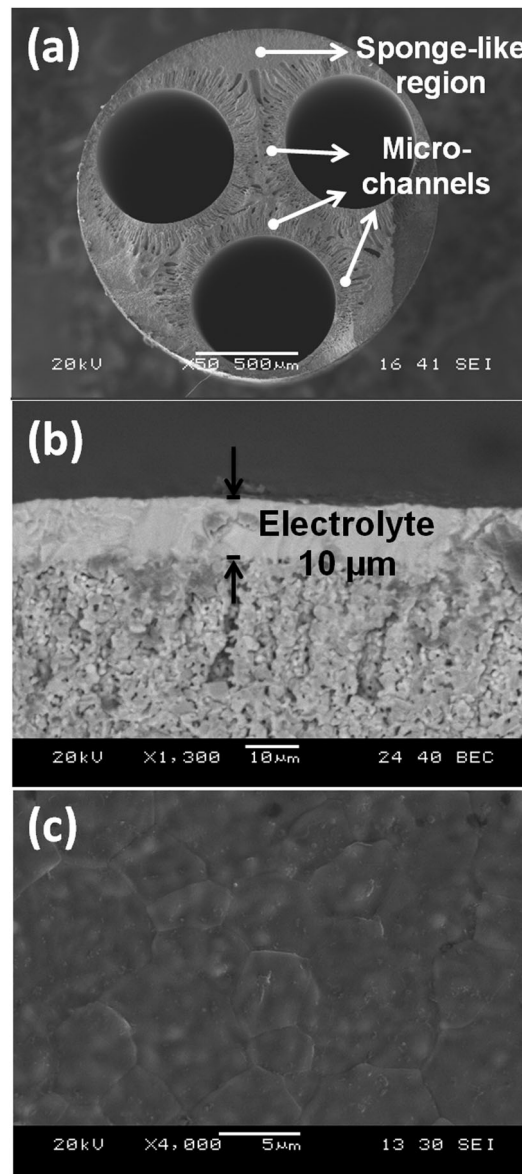


Fig. 2 SEM images of: (a) overview of anode cross-section; (b) close-up of the electrolyte cross-section; (c) close-up of the electrolyte outer surface.

theoretical values, indicating gas-tightness of the YSZ electrolyte. Maximum power densities of 0.09, 0.16 and 0.20 W cm<sup>-2</sup> were determined for air at 650, 700 and 750 °C, respectively, whereas the values were increased significantly to 0.14, 0.20, 0.31 W cm<sup>-2</sup> when air was replaced with N<sub>2</sub>O. Such an increase of up to 50% could be attributed to the improved effective oxygen mass transport due to the catalytic activity of LSM to N<sub>2</sub>O decomposition. Like other SOFCs, here the cathode configuration used a bi-layer structure with a pure LSM outer layer and a LSM–YSZ inner layer. In the case of air, being a pure electronic conductor, the exterior LSM layer functioned mainly as a current collector to transport electrons, but did not contribute to the reduction of air and conduction of oxygen ions. Therefore, air needed to diffuse through the LSM layer, which may act as a barrier for an oxidant to reach the TPBs in the LSM–YSZ composite layer at which



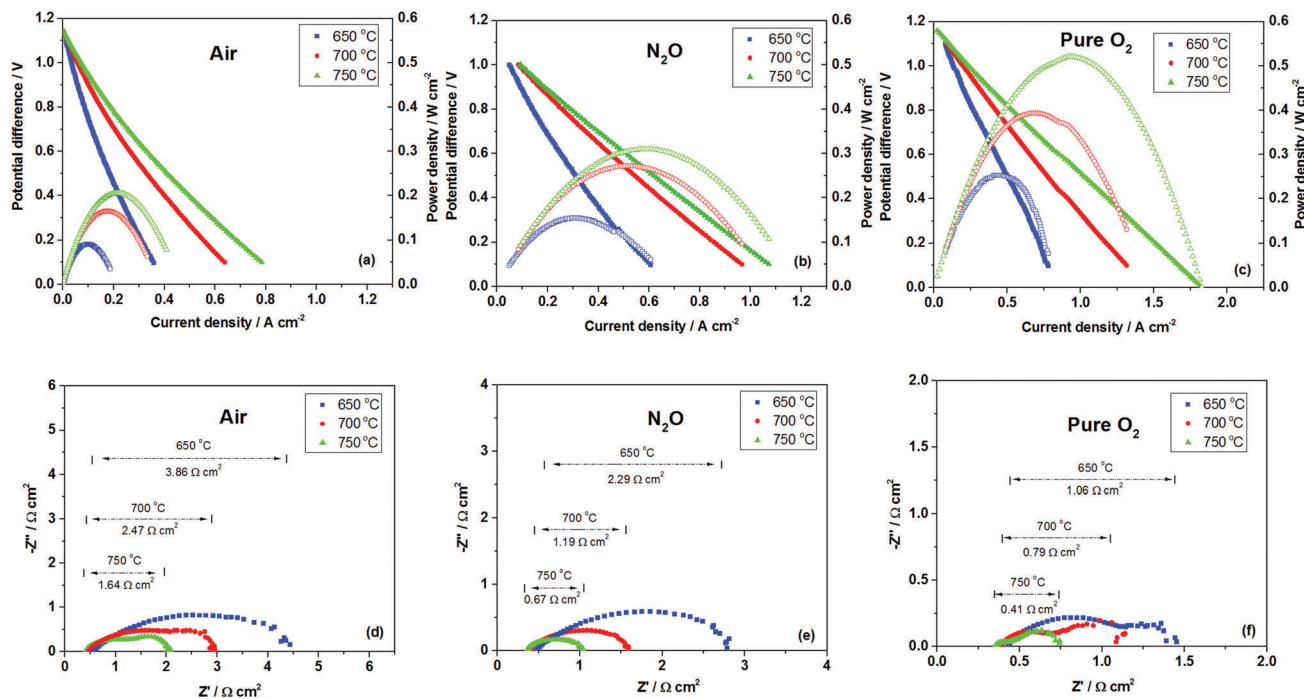


Fig. 3 (a–c) Effects of current density and temperature on cell potential differences with 50 ml min<sup>-1</sup> air, N<sub>2</sub>O or pure O<sub>2</sub>, respectively, as the oxidant and 30 ml min<sup>-1</sup> H<sub>2</sub>; geometric area 0.56 cm<sup>2</sup>. (d–f) Effects of temperature and oxidant type (air, N<sub>2</sub>O, pure O<sub>2</sub> respectively) on impedance spectra for open-circuit conditions.

oxygen was reduced into oxide ions. In contrast, for the N<sub>2</sub>O case, LSM exhibited a significant catalytic activity for N<sub>2</sub>O decomposition, therefore N<sub>2</sub>O would be converted into nitrogen and oxygen in the LSM layer (as confirmed *via* gas chromatography analysis) and in this instance the LSM functioned as an *in situ* oxygen generator. Assuming N<sub>2</sub>O and air have similar transport characteristics in the porous LSM layer, it can be estimated that after decomposition of N<sub>2</sub>O, the local oxygen partial pressure in the LSM layer of the N<sub>2</sub>O case would be up to 238% of the air case, resulting in much more oxygen transport from the LSM layer to the reactive LSM–YSZ layer, and hence, significantly enhancing the reaction in the cathode and the overall performance.

When pure oxygen was investigated as an oxidant, although the LSM layer may also show the resistance for oxygen to reach the TPBs, the pure oxygen contents in the LSM–YSZ composite layer led to a much pronounced effect, resulting in an enhanced performance compared to air and N<sub>2</sub>O as shown in Fig. 3c. Such observation is in good agreement with previous studies in which pure oxygen was tested as an oxidant in comparison to air and exhibited a markedly improved power density and reduced over potential.<sup>27,28</sup> The above results are further supported by the electrochemical impedance spectra which were recorded for temperatures in the range of 650–750 °C under open-circuit conditions, as shown in Fig. 3d–f. As can be seen, with N<sub>2</sub>O as an oxidant, the area specific resistances (ASRs) were measured as 2.29, 1.19 and 0.67 Ω cm<sup>2</sup> at 650, 700 and 750 °C, respectively, which are significantly lower than the electrode polarization of air, but higher than that of pure oxygen, indicating the importance of local oxygen concentration on electrode polarization and hence cell performances.

From the high frequency intercepts on the real impedance ( $x$ ) axis ohmic potential losses were 0.40–0.47 Ω cm<sup>2</sup> when N<sub>2</sub>O was used as the oxidant, whereas the corresponding values for air were 0.47–0.57 Ω cm<sup>2</sup>. This difference could have been due to the local temperature increase of over 30 °C at the cathode (see the ESI† for the experimental results of the temperature change between air/N<sub>2</sub>O, *i.e.* Fig. S5) as a result of the heat released from the exothermic N<sub>2</sub>O decomposition reaction ( $\Delta_r H_{298K}^\circ = -82.05$  kJ mol<sup>-1</sup>) and subsequently increased conductivity.<sup>5</sup>

Considering that pure oxygen is not often used in SOFCs due to it having a much higher cost than air, it is justifiable that air should be the counterpart for techno-economic and performance comparisons with the N<sub>2</sub>O case. Fig. 4 shows the effects of temperature (650–750 °C) on maximum power densities for N<sub>2</sub>O and air, as well as N<sub>2</sub>O conversion data; (neat) N<sub>2</sub>O as the oxidant increased the power densities by up to 50%. Table 1 compares the electrochemical performance results with data reported in the literature for similar materials and operating conditions. The maximum power density for air as the oxidant compares quite well with data for micro-tubular SOFCs reported in the literature. The 50% improvement in N<sub>2</sub>O as the oxidant combined with the enhanced mechanical robustness suggests that this new design and operating condition would be more advantageous over the current state-of-the-art tubular SOFCs. A preliminary stability test has also been conducted at 0.7 V and 750 °C, as shown in Fig. S5 (ESI†).

The highest N<sub>2</sub>O conversion, calculated from gas chromatography data, was 55.6% at 750 °C. Although industrial catalytic or thermal decomposition can achieve > 95% N<sub>2</sub>O removal, it is noteworthy that the conversion reported here resulted from an



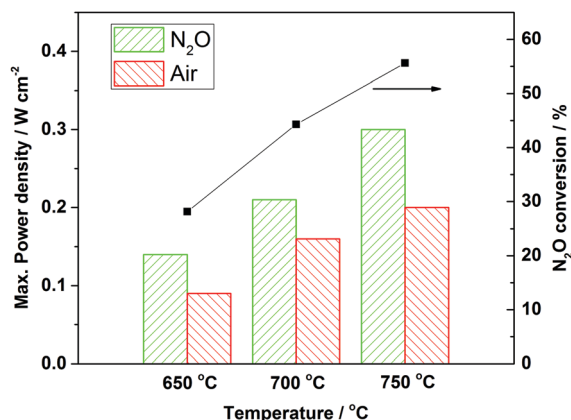


Fig. 4 Effects of temperature and oxidant type (N<sub>2</sub>O or air) on maximum power densities, together with data for N<sub>2</sub>O conversion.

Table 1 Comparison of electrochemical performance for Ni-YSZ|YSZ|YSZ–LSM based tubular solid oxide fuel cells operating on air or N<sub>2</sub>O

Geometry	Temperature/°C	Max. power density/W cm <sup>-2</sup>	Ref.
Single-channel micro-tube	750	0.13	29
	750	0.21	30
	750	0.18	31
	750	0.25	32
	800	0.26	33
	900	0.06	34
Multi-channel micro-tube	750 (air)	0.21	This work
	750 (N <sub>2</sub> O)	0.31	

SOFC with an active cathode length of only 10 mm and a thickness of 30 μm. If SOFC stacks were to be used, to increase the cathode active area, N<sub>2</sub>O conversion could well be increased to match those achieved industrially.

Fig. 5 shows the techno-economic analysis for N<sub>2</sub>O as the oxidant in a 3-channel SOFC (for calculations and assumptions

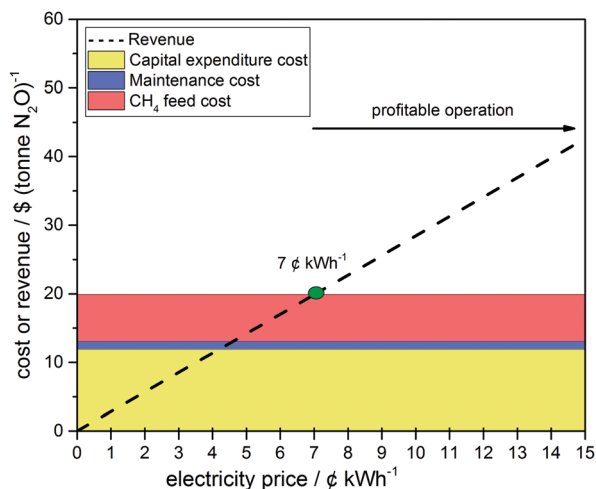


Fig. 5 Effect of electricity price on profitability for electrical energy generation using micro-tubular SOFCs utilizing CH<sub>4</sub> (fuel) and N<sub>2</sub>O (oxidant) operated at 750 °C and 0.31 W cm<sup>-2</sup>.

see the ESI<sup>†</sup>). The fuel chosen was methane, as renewable hydrogen is not yet economically viable with *e.g.* 6.64 \$ kg<sup>-1</sup> for wind-powered electrolysis compared to reforming natural gas 1.03 \$ kg<sup>-1</sup> without CO<sub>2</sub> emission tax.<sup>35</sup> Direct SOFC operation using methane has proven to be viable with a marginal decrease in power density.<sup>18,36,37</sup> The minimum electricity price, at which the capital expenditure, maintenance and methane feed costs are off-set by the revenue from selling the generated electrical energy, was predicted to be *ca.* 0.07 \$ kW h<sup>-1</sup>. Above this price electricity generation using a 3-channel micro-tubular SOFC was predicted to be profitable; with the additional benefit of simultaneously treating N<sub>2</sub>O.

Conventional catalytic decomposition of N<sub>2</sub>O requires high temperatures and catalysts.<sup>38</sup> The SOFC fulfils both these requirements with operating temperatures >600 °C and incorporating a LSM catalyst, while at the same time generating electrical energy. No modification of the SOFC is required for N<sub>2</sub>O operation compared to air. Moreover, as shown in Fig. 3, the N<sub>2</sub>O actually enhances the performance of the SOFC compared to O<sub>2</sub>. Similarly, N<sub>2</sub>O decomposition should benefit, as the product oxygen is removed. Thus, N<sub>2</sub>O treatment at no effective cost penalty can be achieved.

## Conclusions

In summary, this proof-of-concept study demonstrates the feasibility of applying SOFC technology to generate clean electrical energy while simultaneously reducing N<sub>2</sub>O emissions. The novel multi-channel geometric design improved the mechanical strength by 3–4 times that of conventional micro-tubes, which could address the long-existing weakness of single micro-tubular SOFCs and enhance the system resistance towards external impact. Maximum power densities were increased by up to 50% when (neat) N<sub>2</sub>O was used instead of air as the oxidant. The highest power density of 0.31 W cm<sup>-2</sup> was obtained at 750 °C using N<sub>2</sub>O as the oxidant. Electrochemical impedance spectra suggested that the performance improvement was mainly due to decreased polarization as N<sub>2</sub>O decomposition may lead to a more oxygen-rich atmosphere near the cathode surface. The techno-economic evaluation results suggested that this novel conceptual design may well eliminate the cost penalty for industrial N<sub>2</sub>O abatement, provided methane is used as the fuel.

## Acknowledgements

We acknowledge the research funding provided by the UK EPSRC Grant no. EP/M014045/1 and EP/M01486X/1.

## Notes and references

- 1 J. C. Kramlich and W. P. Linak, *Prog. Energy Combust. Sci.*, 1994, **20**, 149–202.
- 2 M. Chipperfield, *Nat. Geosci.*, 2009, **2**, 742–743.
- 3 A. R. Ravishankara, J. S. Daniel and R. W. Portmann, *Science*, 2009, **326**, 123–125.



- 4 P. Forster, V. Ramaswamy, P. Artaxo, T. Berntsen, R. Betts, D. W. Fahey, J. Haywood, J. Lean, D. C. Lowe, G. Myhre, J. Nganga, R. Prinn, G. Raga, M. Schulz and R. Van Dorland, *Changes in Atmospheric Constituents and in Radiative Forcing. In: Climate Change 2007: The Physical Science Basis. Contribution of Working Group I to the Fourth Assessment Report of the Intergovernmental Panel on Climate Change*, Cambridge University Press, Cambridge, United Kingdom and New York, NY, USA, 2007.
- 5 M. Konsolakis, *ACS Catal.*, 2015, **5**, 6397–6421.
- 6 S. J. Hall and P. A. Matson, *Nature*, 1999, **400**, 152–155.
- 7 K. A. Smith and F. Conen, *Soil Use Manage.*, 2004, **20**, 255–263.
- 8 O. Oenema, N. Wrage, G. L. Velthof, W. J. van Groenigen, J. Dolfining and P. J. Kuikman, *Nutr. Cycling Agroecosyst.*, 2005, **72**, 51–65.
- 9 A. Shimizu, K. Tanaka and M. Fujimori, *Chemosphere: Global Change Sci.*, 2000, **2**, 425–434.
- 10 F. Kapteijn, J. Rodriguez-Mirasol and J. A. Moulijn, *Appl. Catal., B*, 1996, **9**, 25–64.
- 11 M. Itakura, Y. Uchida, H. Akiyama, Y. T. Hoshino, Y. Shimomura, S. Morimoto, K. Tago, Y. Wang, C. Hayakawa, Y. Uetake, C. Sanchez, S. Eda, M. Hayatsu and K. Minamisawa, *Nat. Clim. Change*, 2013, **3**, 208–212.
- 12 N. Gao, W. Shen, H. Kakuta, N. Tanaka, T. Fujiwara, T. Nishizawa, N. Takaya, T. Nagamine, K. Isobe, S. Otsuka and K. Senoo, *Soil Biol. Biochem.*, 2016, **97**, 83–91.
- 13 A. Shimizu, K. Tanaka and M. Fujimori, *Chemosphere: Global Change Sci.*, 2000, **2**, 425–434.
- 14 N. Russo, D. Mescia, D. Fino, G. Saracco and V. Specchia, *Ind. Eng. Chem. Res.*, 2007, **46**, 4226–4231.
- 15 S. C. Singhal, K. Kendall and W. Winkler, in *High Temperature Solid Oxide Fuel Cells: Fundamentals, Designs and Applications*, ed. S. C. Singhal and K. Kendall, Elsevier Oxford, UK, 2003.
- 16 R. J. Gorte, *Science*, 2015, **349**, 1290.
- 17 R. Gorte and S. McIntosh, *Chem. Rev.*, 2004, **104**, 4845–4866.
- 18 R. Gorte, J. Vohs and S. Park, *Nature*, 2000, **404**, 265–267.
- 19 T. Suzuki, T. Yamaguchi, K. Hamamoto, Y. Fujishiro, M. Awano and N. Sammes, *Energy Environ. Sci.*, 2011, **4**, 940–943.
- 20 K. Kendall, *Int. J. Appl. Ceram. Technol.*, 2010, **7**, 1–9.
- 21 V. Lawlor, S. Griesser, G. Buchinger, A. G. Olabi, S. Cordiner and D. Meissner, *J. Power Sources*, 2009, **193**, 387–399.
- 22 V. Lawlor, *J. Power Sources*, 2013, **240**, 421–441.
- 23 M. H. D. Othman, N. Droushiotis, Z. Wu, G. Kelsall and K. Li, *Adv. Mater.*, 2011, **23**, 2480–2483.
- 24 T. Suzuki, Z. Hasan, Y. Funahashi, T. Yamaguchi, Y. Fujishiro and M. Awano, *Science*, 2009, **325**, 852–855.
- 25 T. Li, Z. Wu and K. Li, *J. Power Sources*, 2015, **280**, 446–452.
- 26 L. Kleiminger, T. Li, K. Li and G. H. Kelsall, *RSC Adv.*, 2014, **4**, 50003–50016.
- 27 E. P. Murray, T. Tsai and S. A. Barnett, *Solid State Ionics*, 1998, **110**, 235–243.
- 28 M. C. Tucker, G. Y. Lau, C. P. Jacobson, L. C. DeJonghe and S. J. Visco, *J. Power Sources*, 2007, **171**, 477–482.
- 29 T. Suzuki, M. Awano, P. Jasinski, V. Petrovsky and H. Anderson, *Solid State Ionics*, 2006, **177**, 2071–2074.
- 30 M. Kendall, A. D. Meadowcroft and K. Kendall, *ECS Trans.*, 2013, **57**, 123–131.
- 31 N. Droushiotis, A. Hankin, C. Rozain and G. H. Kelsall, *J. Electrochem. Soc.*, 2013, **161**, F271–F279.
- 32 C. Ren, T. Liu, Y. Mao, P. Maturavongsadit, J. A. Luckanagul, Q. Wang and F. Chen, *Electrochim. Acta*, 2014, **149**, 159–166.
- 33 C. Jin, C. Yang and F. Chen, *J. Membr. Sci.*, 2010, **363**, 250–255.
- 34 T. Mahata, S. R. Nair, R. K. Lenka and P. K. Sinha, *Int. J. Hydrogen Energy*, 2012, **37**, 3874–3882.
- 35 T. Abbasi and S. A. Abbasi, *Renewable Sustainable Energy Rev.*, 2011, **15**, 3034–3040.
- 36 R. Gorte, J. Vohs, S. Park and C. Wang, *Adv. Mater.*, 2000, **12**, 1465–1469.
- 37 J.-H. Koh, Y.-S. Yoo, J.-W. Park and H. C. Lim, *Solid State Ionics*, 2002, **149**, 157–166.
- 38 O. o. A. Q. P. a. S. Sector Policies and Programs Division, U.S. Environmental Protection Agency, Research Triangle Park, North Carolina 27711 *Available and Emerging Technologies for Reducing Greenhouse Gas Emissions from the Nitric Acid Production Industry* 2010.

